Metrol. Meas. Syst., Vol. 31 (2024), No. 2
DOI: 10.24425/mms.2024.149699

METROLOGY AND MEASUREMENT SYSTEMS
Index 330930, ISSN 0860-8229
www.metrology.wat.edu.pl

EVALUATING METROLOGICAL PERFORMANCE OF A PRESSURE BALANCE UTILIZING A HIGH-PRECISION FORCE TRANSDUCER: AN EXPERIMENTAL STUDY

Shaker A. Gelany, Gouda M. Mahmoud

National Institute of Standards (NIS), Tersa St, El-Haram, PO Box 136, Code 12211, Giza, Egypt (✉ *shaker9595@yahoo.com*)

Abstract

This paper describes the development and evaluation of a force-pressure balance system utilizing a high-precision force transducer. This setup aims to calibrate hydraulic pressure gauges commonly used in industrial applications, with a measurement range of up to 50 MPa. Detailed investigations were conducted to determine the metrological characteristics and calibration coefficients of the new force-pressure balance setup. Comparisons were made between the results obtained from the new setup and those obtained from another reference pressure standard. The findings highlighted a decrease in the accuracy of the pressure balance within the lower pressure range. This decrease in accuracy can be attributed to the hysteresis effect caused by the force transducer utilized in the setup. Additionally, an error was observed in the pressure characteristic of the piston's performance, particularly in the lower pressure range. These findings indicate the need for further improvements in the force-pressure balance system to enhance accuracy across the entire pressure range.

Keywords: piston gauge, porce pressure balance, pressure balance, force transducer, cross-floating.

1. Introduction

Many industrial applications, such as nuclear power, gas, automotive, and process control, are highly dependent on pressure measurements. Moreover, due to the advancing technology of pressure measuring instruments in scientific and manufacturing applications, there is a growing need for higher accuracy in calibration devices [1–4]. The growing market for high-precision force transducers, along with the advancements in digital amplifiers and processing units, has given weighing instrument manufacturers the ability to create dynamometers with exceptional performance. These instruments demonstrate linearity and repeatability that surpass one part per million of the full scale. As a result, the traditional force measurement method needs to be reconsidered. The combined utilization of a piston cylinder and an electronic dynamometer presents a compelling advancement in force measurement. This system offers accuracy comparable to traditional methods, which use mass as the measuring standard, while also providing the advantages of electronic instrumentation. This instrument eliminates the laborious task of handling masses, provides a digital display, and can be connected to data acquisition systems. As a result, many users who currently rely on transfer standards now have access to a portable digital standard. Researchers in the field of pressure metrology have presented various designs of digital readout pressure standards. In 1994, A. Ooiwa [5] developed a new type of piston gauge to address the challenges associated with classical piston gauges in measuring small differential pressure. Classical piston gauges require balancing the pressure against the weight of the piston, which often corresponds to several kilopascals of pressure. Additionally, minimizing pressure fluctuations caused by piston or cylinder rotation to below 0.1 Pa is also difficult. Ooiwa's novel piston gauge

Article history: received November 04, 2023; revised February 2, 2024; accepted February 6, 2024; available online March 18, 2024.

overcomes these issues and allows for the measurement of small differential gas pressures ranging from 1 Pa to 10 kPa with a sensitivity of approximately 5 mPa. This piston gauge employs two distinct functionalities, with one compensating for the weight of the piston and the other ensuring the piston's centralization within the cylinder without any rotational movement. With these mechanisms in place, an electronic balance can measure the force exerted on the piston by a small differential pressure. C. G. Rendle [6] designed a large-area piston gauge capable of measuring pressures ranging from zero to 3.2 kPa. This innovative mechanism securely positions a sizable piston at the center of the cylinder, eliminating the need for friction or rotation. Additionally, the piston system is connected to an electronic balance, enabling direct measurements in pascals. In their research paper, L. Dargent from Desgranges et Huot presented a digital piston manometer (used for calibrating pneumatic pressures) [7]. The author primarily focuses on explaining the technical principles of the digital readout piston-cylinder type, which serves as a pressure standard. Furthermore, the paper discusses its classification as a primary pressure standard based on its nature. The research also includes recent evaluation results, highlighting the exceptional measurement specifications of the digital piston manometer. These results demonstrate that the digital readout piston-cylinder can be reliably used as a transfer standard with minimal degradation in accuracy over time. Jasveer Singh from NPLI [8], the National Physical Laboratory of India, conducted a research study on the stability of a digital pressure gauge operating in the range of 60 bar over nine years. The study aimed to analyze the impact of various factors, such as repeatability, hysteresis, non-linearity, and relative deviation, on the stability of the gauge. A comprehensive analysis was performed for each of these factors. The results revealed that the equipment consistently performed well for approximately 5 years before a slight shift occurred in the aforementioned parameters. Despite this slight alteration, the overall performance of the equipment remained outstanding throughout the entire study period, taking into account any experimental uncertainties.

This study aims to present the development of a loading mechanism that offers an alternative to using masses in classical hydraulic pressure balances. This loading mechanism will enable a high-precision force transducer to be connected with a piston-cylinder assembly, providing a solution for applications where commercial instruments do not meet the required range (50 MPa), transmitting medium (hydraulic), and accuracy (60 ppm). To achieve this aim, a metrological study of the *force pressure balance* (FPB) will be conducted. This study will involve conducting individual calibrations for all system components, ensuring their accuracy and reliability. Additionally, the results obtained from the FPB will be compared with those of another pressure reference standard within the range of up to 50 MPa, providing a comprehensive evaluation of the loading mechanism's performance.

2. Basic principles of pressure balance

The classical pressure balance, as depicted in Fig. 1a, consists of the mass set and the piston-cylinder assembly. The principle of the pressure balance depends on direct pressure measurement through the force exerted by a known mass, under the influence of acceleration due to gravity, onto a surface of a known area. In practical implementations, a pressure-transmitting fluid, typically oil or gas, is employed to exert pressure on the base of a piston, which is free to move within a precisely matched cylinder (upward force). The resulting upward force is counterbalanced by a known downward force generated by calibrated masses positioned atop the piston, with local gravitational acceleration taken into account, as exemplified in the (1) [4, 9].

$$\sum m.\, g = p.\, A_p \tag{1}$$

Metrol. Meas. Syst., Vol. 31 (2024), No. 2
DOI: 10.24425/mms.2024.149699

The combined utilization of a piston cylinder and a force transducer introduces a novel pressure standard known as the FPB. In contrast to the classical pressure balance method, where a piston is loaded with masses, this approach (FPB) allows for the calibration of the force transducer using masses. When the piston is vertically moved and positioned on the force transducer, it enables continuous interpolation of force measurements, as demonstrated in Figure 1b. [5, 10].

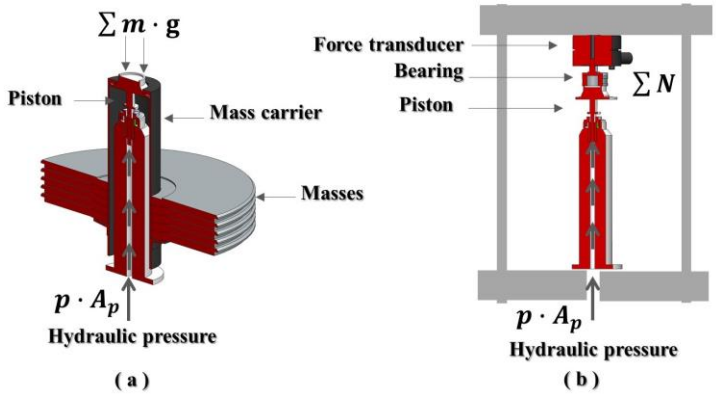

Fig.1. The basic operating concept: (a) Classical pressure balance (b) Force pressure balance.

3. Experimental layout

The force-pressure balance setup consists of three main components: a loading frame, a hydraulic pressure generator (pump), and the channel of the unit under calibration. Figure 2 illustrates the experimental arrangement of this setup. The unit under calibration is positioned on the left side and connected to the loading frame through a short tubing. Shut-off valve 2 is used to separate the loading frame and the calibration unit from the hydraulic pump. The hydraulic pump supplies pressurized fluid to both the loading frame and the unit under calibration. The reservoir is used to fill the hydraulic pump before calibration, and after that, shut-off valve 1 isolates the pump from the ambient pressure.

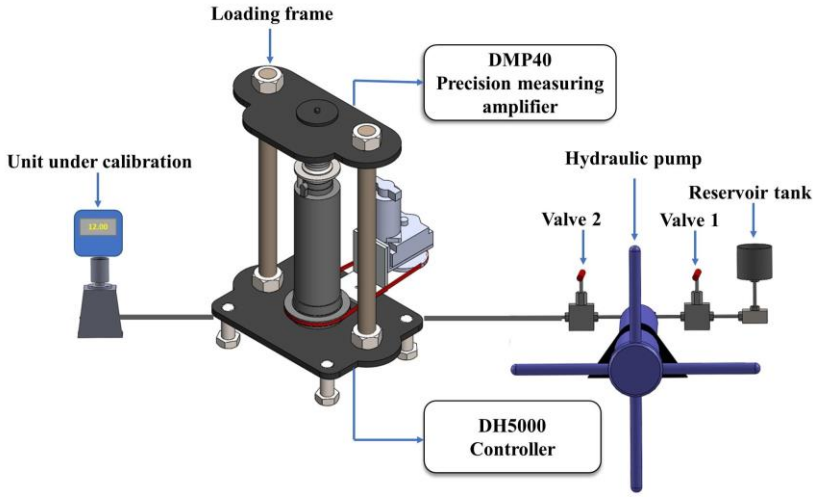

Fig.2. Layout of the hydraulic force pressure balance.

3.1. Loading Frame

Figure 3 illustrates an exploded view drawing of the loading frame used in the FPB, along with its assembly view. The loading frame comprises several components, including an upper plate, a lower plate, two rods, and a mounting post. The mounting post is a column made of stainless steel on which a pulley is fixed with bearings. A drive belt allows a motor to turn the pulley. Furthermore, the mounting post is securely installed vertically on the lower plate. Pressure is converted into a measurable, proportional force by the *piston-cylinder assembly* (PCA). The PCA (manufactured by Desgranges et Huot) is positioned vertically within the mounting post. To make precise temperature corrections, the temperature probe is positioned as close as possible to the piston cylinder on the mounting post. The temperature is then displayed through a Desgranges et Huot DH5000 controller. The force transducer is installed on the upper plate of the loading frame. The piston enables continuous force measurement interpolation when positioned on the force transducer. The force transducer measures the upward force that the piston produces when moving vertically, and it is capable of measuring forces up to 10 kN. HBM's precision measuring amplifier, model number DMP40, is used to indicate the force transducer's readings. A thrust ball bearing is employed as a coupling between the piston-cylinder and the force transducer. The thrust ball bearings consist of two bearing washers: one washer is fixed on the piston head, and the other washer is fixed on the force transducer. These washers are accompanied by a cage containing the balls. The main function of a thrust ball bearing is to accommodate the axial loads of the piston, ensuring accurate positioning of the piston and compensating for misalignment between the piston's axis and the force transducer's measuring axis. Simultaneously, it helps maintain low friction and reduce any remaining vibrations resulting from the rotation of the piston. The piston rotates by utilizing a pin fixed on a pulley, which pushes another pin located on the piston head. The motor rotates the pulley by using a drive belt. The motor speed is set at 30 rpm to minimize pressure fluctuations resulting from piston rotation, ensuring a consistently stable and repeatable readout.

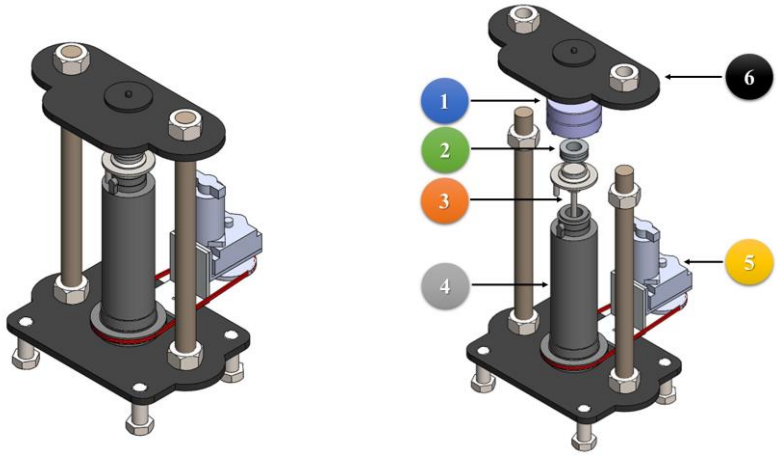

Fig. 3. The assembly view and the exploded view of the FPB loading frame: 1. Force transducer, 2. Thrust ball bearing, 3. Piston, 4. Mounting post, 5. DC motor, 6 Frame upper plate.

4. Force pressure balance theory

In contrast to the classical pressure balance system, where a piston is loaded with masses, the force-pressure balance system allows for calibrating the force transducer using masses. When the piston is vertically moved and positioned on the force transducer, it enables continuous interpolation of force measurements. A force-pressure balance system measures

pressure by analyzing the various force components applied to the system. The equation for pressure in a classical pressure balance system serves as the basis for computing pressure using a force-pressure balance system. For a force-pressure balance, the pressure is measured given by [9]:

$$F_{cal} + F_p + F_c = p.A, \tag{2}$$

where F_{cal} represents the force transducer calibration coefficients, which are explained in detail in Section 5.1 of this paper. F_p denotes the force attributed to the piston mass, including the mass of the thrust ball bearing. Moreover, F_c represents the force caused by fluid surface tension. To ensure accurate calculation of pressure values measured by the FPB, corrections are necessary. It is essential to correct the mass of the piston gauges due to the air buoyancy effect in order to obtain precise measurements. Air buoyancy refers to the upward force exerted by the ambient air, which counteracts the mass of the piston. Equation (3) should be used to correct the piston mass value.

$$F_p = m_p \left(1 - \frac{\rho_a}{\rho_p}\right).g, \tag{3}$$

where ρ_a represents air density, m_p represents the mass of the piston, ρ_p represents the density of the piston, and g represents the local acceleration due to gravity.

The term 'force due to surface tension' acts at the perimeter of the piston. The force of fluid surface tension needs to be corrected using (4).

$$F_c = \gamma.C, \tag{4}$$

where γ represents the surface tension of the fluid and *C* denotes the circumference of the floating element of the assembly at the point where it emerges from the pressure fluid.

In (2), the right-hand side signifies the force that arises from fluid pressure *p* acting on the effective area of the PCA. This effective area can be described as follows [9, 11]:

$$A = A_p[1 + (\alpha_p + \alpha_c)\ t - 20\ ], \tag{5}$$

where *A* is the corrected effective area, A_p is the effective area at the reference temperature, which is explained in detail in section 5.2. *t* represents the temperature of PCA during the measurement, whereas α_p and α_c denote the thermal expansion coefficients of both the piston and cylinder. By utilizing equations (2), (3), (4), and (5), the pressure can be represented as (6):

$$p = \frac{F_{cal}+F_p+F_c}{A_p[1+(\alpha_p+\alpha_c)\ t-20\ ]}. \tag{6}$$

5. Metrological study

A metrological study of the force-pressure balance was conducted through a series of individual calibrations for all system components. Additionally, the results of the system were compared with those of another pressure reference standard. The *calibration and measurement capabilities* (CMC) of this pressure reference standard are published in the *Key Comparison Database* (KCDB) of the *Bureau International des Poids et Mesures* (BIPM) [12].

5.1. Calibration of the force transducer

The high-precision force transducer was calibrated according to ISO/IEC 376:2011 [12, 13]. A set of disk masses are used to calibrate the high-precision force transducer. These disk

masses were calibrated with a relative expanded uncertainty of 1.8×10^{-6}. The force transducer calibration setup is shown in Fig. 4.

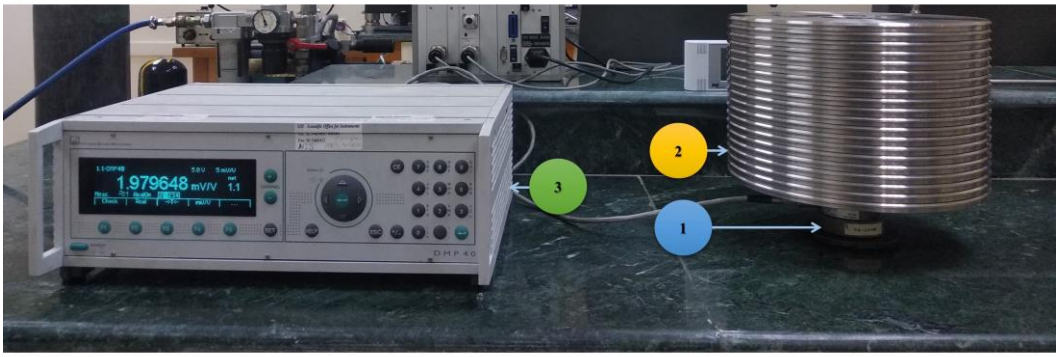

Fig. 4. The force transducer calibration setup:
1. Force transducer, 2. Disk masses, 3. precision amplifier DMP40.

The output values of the force transducer were determined at each calibration point using the provided (7) [15]. The reference force was calculated for each applied point.

$$F_r = m_i\left(1 - \frac{\rho_a}{\rho_{mi}}\right).g, \tag{7}$$

where F_r is the reference force, *mi* is the individual mass value of each disk mass, *g* is the local gravitational acceleration, ρ_a is the density of air, and ρ_{mi} is the density of each disk mass.

The Humlog 20 data logger is used to measure the ambient pressure, temperature, and humidity during calibrations. Consequently, the air density ρ_a and its associated uncertainty were calculated accordingly [16], The results of the air density are 1.1939±0.12 kg.m^{-3}. The density of disk masses ρ_{mi} and its standard uncertainty are according OIML R 111-1 [16] for stainless steel alloy. Therefore, the density of disk masses and its standard uncertainty are 7920±140 kg.m^{-3}. The local acceleration due to gravitational *g* were measured at the FPB's location and was found as $9.79299022 \pm 2\times10^{-8}$ m.s^{-2}. The calibration coefficients of the force transducer were calculated using the least square regression method according to the polynomial (8). According to force proving instrument calibration methods like ASTM E 74 and ISO 376:2011[13,17], a polynomial equation is fitted to the calibration data using the least squares method to predict deflection values throughout the entire loading range. This method is well-known for its accuracy in capturing the interpolation effect.

$$F_{cal} = a.R + b.R^2, \tag{8}$$

where *a, b* are the constants of the calibration equation, and *R* is the response of the force transducer (mV/V).

5.2. Calibration of piston cylinder assembly

One of the essential parts in constructing any pressure balance system is the piston-cylinder assembly. The piston-cylinder assembly of the FPB was calibrated following the EURAMET CG-3 guideline [9-11]. The piston-cylinder assembly of the FPB was calibrated by direct comparison (cross float) with another reference pressure balance to determine the calibration coefficients. The basics of the cross-float method consist of balancing the pistons of two pressure balances bound by the same pressure line at a specific pressure value. To achieve this balance, trim masses are added or removed until the piston gauges are in

equilibrium. In the state of equilibrium, the ratio of the corrected effective areas of the two piston-cylinder units correspond to the ratio of the corrected loads.

The pressure at the reference level, p^R is affected by air buoyance due to air density and the average density of used masses $(1-\rho_a/\rho_m\ )$, the thermal expansion coefficients of the piston and cylinder materials $(\alpha_p+\alpha_c\ )$, the temperature of the piston (*t*), and the pressure distortion coefficient of the piston cylinder assembly (λ), in addition to the sum of the forces resulting from the masses used, including the mass of the piston due to acceleration gravity and piston effective area $(\sum m \bullet \mathrm{g})$. The mathematical model of the pressure generated for the piston gauge in (9) takes the above-mentioned factors into account [9, 11 ,19].

$$p^R = \frac{\sum m.g\left(1-\frac{\rho_a}{\rho_m}\right)}{A_0\ 1+\lambda.p\ [1+(\alpha_p+\alpha_c)\ t-20\ ]} \pm \rho_f.\, g.\, h. \tag{9}$$

The effective area of the FPB's as a function of pressure A_p^T, can be obtained as follow.

$$A_p^T = \frac{\sum m_i^T.g\left(1-\frac{\rho_a}{\rho_{mi}^T}\right)+\sigma^T.C^T}{p^R[1+(\alpha_p^T+\alpha_c^T)\ t-20\ ]}, \tag{10}$$

where m_i^T are true masses of the FPB's piston, the mass carrier, and the mass pieces placed on the mass carrier; ρ_{mi}^T are densities of the parts with masses m_i^T; ρ_a is the air density; *g* is the local gravity acceleration; γ is the surface tension of the oil used; C^T is the nominal circumference of the FPB's piston; p^R is the pressure generated by the reference pressure balance at the FPB's reference level; α_p^T and α_c^T are thermal expansion coefficients of the piston and cylinder materials, respectively; *t* is the temperature of the FPB's piston. The effective area at zero pressure A_0 and the distortion coefficient λ can be obtained as the following form.

$$A_p = A_0\ 1+\lambda.p\ +\frac{\Gamma}{p} \tag{11}$$

The coefficient for above form is obtained from a polynomial regression fit.

5.3. Metrological verification of the FPB

The results of the FPB as an independent system were compared with those of another pressure reference standard to verify its results. The FPB was measured in five series against the *National Institute of Standards* (NIS) reference pressure balance. Each series comprised 10 pressure points in the rising direction and 10 pressure points in the falling direction. The applied pressure points were (5, 10, 15, 20, 25, 30, 35, 40, 45, and 50) MPa. The pressure values of the FPB at the reference level can be obtained using (6). The experimental setup was established to calibrate the FPB as shown in Fig. 5. In this setup, the FPB is connected to the reference pressure balance. Both systems are cross floated to the selected applied pressure points.

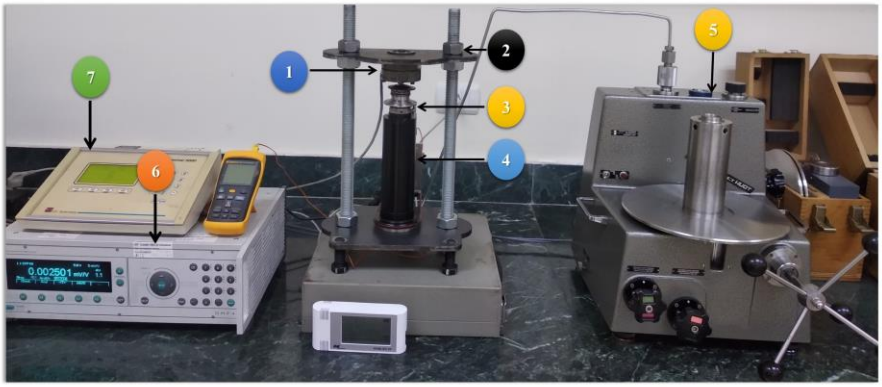

Fig. 5 Experimental setup of comparing FPB system with another standard pressure balance:
1. Force transducer, 2. Frame, 3. Piston, 4. Mounting post, 5. Reference pressure balance, 6 DMP40, 7. Terminal of piston gauge

6. Experimental results

The force transducer was calibrated in 10 % increments with respect to the full-scale value. The force transducer has been preloaded to the maximum range three times in the 0° position. At each calibration point, six sets of measurements were taken. Two sets of measurements were taken at the 0° position in increasing directions. At 120° and 240°, two series of measurements were carried out in both increasing and decreasing directions. Fig. 6 a illustrates the calibration results for the force transducer, displaying the interpolation curve of the results. The x-axis represents the average response of the force transducer, while the y-axis displays the reference force. The calibration function (F_{cal}) was determined employing polynomial regression fit using equation (8). Fig. 6 b shows the interpolation error and the uncertainty of the force measurements. The results show that the relative error is highest in the low range, with a value of 0.009%, and decreases as the measurement range increases. The uncertainty of the force measurement was calculated, and it was found that the largest value observed was 0.008%.

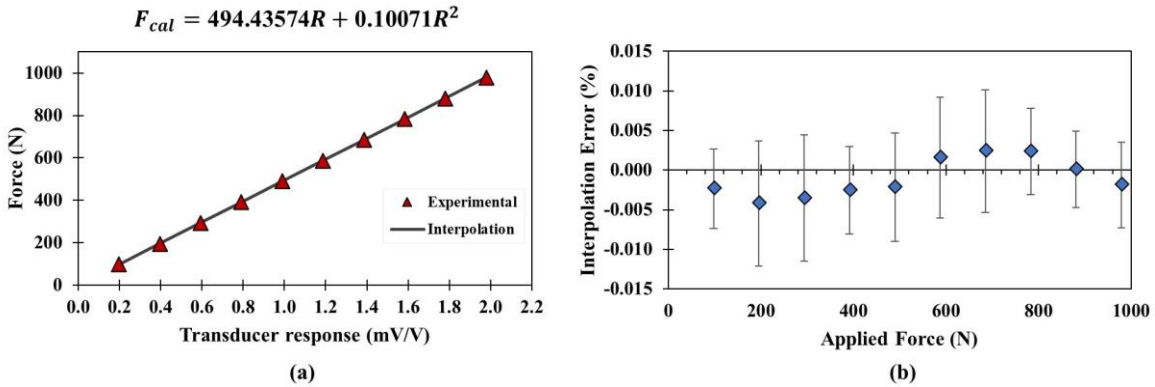

Fig. 6. Calibration results for the force transducer: (a) experimental transducer response (b) Interpolation error

The piston-cylinder assembly was calibrated in three series to determine the calibration curve of the effective area. Each series consisted of ten pressure points in ascending and descending directions. The pressure points were 5, 10, 15, 20, 25, 30, 35, 40, 45, and 50 MPa. Fig. 7 illustrates the results of the calibration for the piston-cylinder assembly. The x-axis displays the average pressures, while the y-axis displays the average areas of the piston-cylinder assembly. Fig. 7 also shows the calibration curve of the piston-cylinder assembly

(A_p). This calibration curve is described by two constants: A_0, the effective area at zero pressure, which is 19.6115 mm²; and λ, the pressure distortion coefficient, which is 4.50×10^{-7} MPa^{-1}. Additionally, there is a tare coefficient of 3.03 kPa, indicating an error in the low-pressure characteristic of the FPB piston's performance. Error bars are used to represent the uncertainty of the calibrated effective areas. At a confidence level of k = 1, it was determined that the relative uncertainty was 32 ppm.

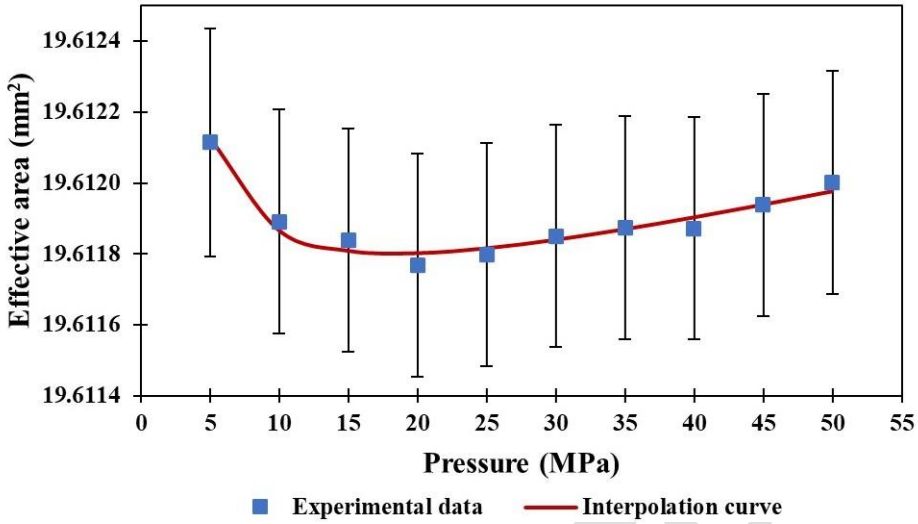

Fig.7 FPB's piston gauge effective area with the estimated uncertainty

The results of the FPB were verified by calibration against the reference pressure balance of NIS, which is recognized internationally by the International Bureau of Weights and Measures. The metrological characteristics of the FPB are presented in table 1.

Table 1. Metrological characteristics of the FPB

Reference Values	FPB Values	Deviation	Repeatability	Hysteresis	Expanded uncertainty
(MPa)	(MPa)	(MPa)	(%)		
4.993350	4.993839	0.000489	0.001	0.035	0.007
9.986529	9.986386	-0.000143	0.004	0.026	0.010
14.979672	14.980511	0.000839	0.004	0.025	0.010
19.972771	19.974790	0.002018	0.005	0.025	0.012
24.965836	24.968914	0.003079	0.006	0.020	0.012
29.958850	29.962701	0.003851	0.006	0.020	0.013
34.951817	34.956042	0.004226	0.005	0.015	0.012
39.944728	39.948932	0.004204	0.005	0.011	0.011
44.937617	44.942337	0.004720	0.005	0.005	0.011
49.930450	49.937009	0.006560	0.005	0.000	0.011

The results show a deviation of the values of the FPB from the reference values. This deviation increases with the increase in the pressure value. The observed results disclosed a maximum repeatability error of 0.006%. Additionally, the hysteresis relative errors were found to be 0.035% and 0.005% at the minimum and maximum ranges, respectively. The expanded uncertainty of the measurement was also calculated and found to be 0.013%.

7. Conclusions

A dedicated loading frame has been developed to connect a high-precision force transducer with a piston-cylinder assembly, offering an alternative to using masses in classical pressure balances. A metrological study of the FPB was conducted, involving a series of individual calibrations for all system components. The high-precision force transducer was calibrated using reference masses based on ISO/IEC 376:2011, with the coefficients of the force calibration function determined for the transducer. The observed results showed a maximum relative interpolation error of 0.009% and a maximum relative uncertainty of 0.008%. The piston-cylinder assembly was calibrated using the cross-floating method, and the coefficients of its calibration function were determined as well. The observed results revealed that the effective area at zero pressure is 19.6115 mm^2 with a relative uncertainty of 32 ppm. The pressure distortion coefficient is 4.50×10^{-7} MPa^{-1}. Additionally, an error in the low-pressure characteristic of the piston performance was observed, with a value of 3 kPa. Furthermore, the results of the FPB were compared with those of another pressure reference standard in the range of up to 50 MPa. The observed results disclosed a maximum repeatability error of 0.006%, while the hysteresis relative errors at the minimum and maximum ranges are 0.035% and 0.005% respectively. The expanded uncertainty of the measurement was also calculated and found to be 0.013%. Hence, the results showed a decreased accuracy in pressure balance, which can be attributed to the hysteresis effect caused by the use of the force transducer. Furthermore, during the evaluation of the piston performance, an error was observed in its pressure characteristic, specifically in the lower pressure range. This discrepancy can be attributed to the pressure fluctuations that occur while the piston rotates.

In the future, an automatic FPB system will be built that utilizes a weighing cell instead of a force transducer. Additionally, another piston-cylinder assembly will be employed. The linearity and hysteresis of both the weighing cell and piston-cylinder assembly will be examined, considering the piston alignment and the impact of piston rotation on the weighing cell. Uncertainty and error sources in the new system will be calculated, and a comprehensive evaluation will be conducted by comparing it to an appropriate standard pressure balance to achieve the anticipated performance.

Acknowledgements

This work has been supported by the National Institute of Standards (NIS), Egypt, through the use of its lab facilities. The support is highly appreciated.

References

[1] Salminen, J., Saxholm, S., Hämäläinen, J., & Högström, R. (2020). Advances in traceable calibration of cylinder pressure transducers. *Metrologia*, *57*(4), 045006. https://doi.org/10.1088/1681-7575/ab8fb9

[2] Thakur, V. N., Yadav, S., & Kumar, A. (2021). Process and insight of Pascal traceability. *MAPAN-Journal of Metrology Society of India*, *36*(3), 691–708. https://doi.org/10.1007/s12647-021-00447-z

[3] Chernyshenko, A. A. (2019). Current state and prospects of development of the reference base in the field of measurements of low absolute pressures and vacuum. *Journal of Physics: Conference Series*, *1313*(1), 012012. https://doi.org/10.1088/1742-6596/1313/1/012012

[4] Rab, S., Yadav, S., & Haleem, A. (2022). A laconic capitulation of high pressure metrology. *Measurement*, *187*, 110226. https://doi.org/10.1016/j.measurement.2021.110226

[5] Ooiwa, A. (1994). Novel Nonrotational Piston Gauge with Weight Balance Mechanism for the Measurement of Small Differential Pressures. *Metrologia*, *30*(6), 607–610. https://doi.org/10.1088/0026-1394/30/6/012

[6] Rendle, C. G. (1994). A Large Area Piston Gauge for Differential and Gauge Pressure from Zero to 3,2 kPa. *Metrologia*, *30*(6), 611–613. https://doi.org/10.1088/0026-1394/30/6/013

[7] Dargent, L. (1994). Digital Piston Manometers: Are they Primary or Transfer Standards? *Metrologia*, *30*(6), 659–663. https://doi.org/10.1088/0026-1394/30/6/022

[8] Singh, J., Kumar, A., Sharma, N. D., & Bandyopadhyay, A. K. (2011). Reliability and long term stability of a digital pressure gauge (DPG) used as a standard- a case study. *MAPAN-Journal of Metrology Society of India*, *26*(2), 115–124. https://doi.org/10.1007/s12647-011-0012-7

[9] Dadson, R. S., Lewis, S. L., & Peggs, G. N. (1982). The pressure balance: Theory and practice, HMSO, London

[10] Ooiwa, A. (1994). Novel Nonrotational Piston Gauge with Weight Balance Mechanism for the Measurement of Small Differential Pressures. *Metrologia*, *30*(6), 607–610. https://doi.org/10.1088/0026-1394/30/6/012

[11] EURAMET (2011). Calibration of Pressure Balances.

[12] BIPM, BIPM, Https://Www.Bipm.Org/Kcdb/Cmc/ (2023).

[13] International Organization for Standardization. (2018). *Metallic materials — Calibration of force-proving instruments used for the verification of uniaxial testing machines* (ISO Standard No. 376:2011). https://www.iso.org/standard/44661.html

[14] Mahmoud, G. M., & Gelany, S. A. (2021). An Investigation on using Lagrange, Newton and Least Square Methods for Generating Nonlinear Interpolation Function for the Measuring Instruments. *ASM Science Journal*, *14*, 1–8. https://doi.org/10.32802/asmscj.2020.702

[15] Dadson, R. S., Lewis, S. L., & Peggs, G. N. (1982). The pressure balance: Theory and practice, HMSO, London

[16] International Organization of Legal Metrology. (2004). *Weights of classes E1, E2, F1, F2, M1, M1-2, M2, M2-3 and M3 Part 1: Metrological and technical requirements* (OIML R 111-1). https://www.oiml.org/en/files/pdf_r/r111-1-e04.pdf

[17] ASTM International, ASTM E74-18E1, Standard Practices for Calibration and Verification for Force-Measuring Instruments, n.d. https://doi.org/10.1520/E0074-18E01

[18] Gelany, S. A., & Sayed, B. M. (2021). Case study on the non-linear behavior of the NIS-50 MPa pressure balance. *Measurement*, *172*, 108865. https://doi.org/10.1016/j.measurement.2020.108865

[19] International Organization of Legal Metrology. (1994). *Pressure balances* (OIML R 110). https://www.oiml.org/en/files/pdf_r/r110-e94.pdf

Shaker A. Gelany received the Ph.D. degree in Mechanical Design and Production Engineering, Faculty of Engineering, Cairo University, in 2019. He is currently a researcher in Mass, Density and Pressure Metrology, National Institute of Standards (NIS), Egypt.

Gouda M. Mahmoud received the Ph.D. degree in Mechanical Design and Production Engineering, Faculty of Engineering, Cairo University, in 2014. He is currently Associate professor of Force & Material Metrology, National Institute of Standards (NIS), Egypt